JOC The Journal of Organic Chemistry

Featured Article

pubs.acs.org/joc

Salinipostins A–K, Long-Chain Bicyclic Phosphotriesters as a Potent and Selective Antimalarial Chemotype

Christopher J. Schulze,[†,§] Gabriel Navarro,[†,§] Daniel Ebert,[‡,§] Joseph DeRisi,*[,‡] and Roger G. Linington*[,†]

[†]Department of Chemistry and Biochemistry, University of California, Santa Cruz, California 95064, United States

[‡]Department of Biochemistry and Biophysics, University of California, San Francisco, California 94158, United States

Supporting Information

ABSTRACT: Despite significant advances in antimalarial chemotherapy over the past 30 years, development of resistance to frontline drugs remains a significant challenge that limits efforts to eradicate the disease. We now report the discovery of a new class of antimalarials, salinipostins A–K, with low nanomolar potencies and high selectivity indices against mammalian cells (salinipostin A: *Plasmodium falciparum* EC_{50} 50 nM, HEK293T cytotoxicity EC_{50} > 50 μM). These compounds were isolated from a marine-derived *Salinospora* sp. bacterium and contain a bicyclic phosphotriester core structure, which is a rare motif among natural products. This scaffold differs significantly from the structures of known antimalarial compounds and represents a new lead structure for the development of therapeutic targets in malaria. Examination of the growth stage specificity of salinipostin A indicates that it exhibits growth stage-specific effects that differ from compounds that inhibit heme polymerization, while resistance selection experiments were unable to identify parasite populations that exhibited significant resistance against this compound class.

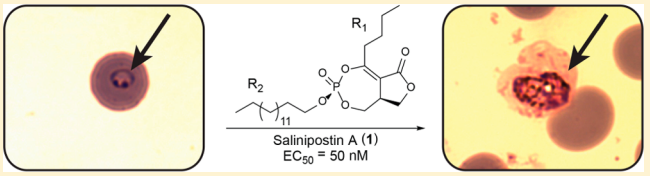

INTRODUCTION

Despite significant efforts toward the eradication of malaria, this vector-borne disease continues to be a major source of morbidity and mortality, particularly in Sub-Saharan Africa, where it imparts a devastating socioeconomic burden.[1] A recent survey by the World Health Organization estimates that there were 216 million cases of malaria in 2010, mostly affecting children under 5 years of age.[2] The causative agents are eukaryotic intracellular parasites of the genus *Plasmodium*, of which *Plasmodium falciparum* causes the most severe form. Disease progression begins with an asymptomatic proliferation phase in the liver, followed by release into the bloodstream where parasites invade and replicate within host erythrocytes. Subsequent egress and reinvasion of erythrocytes results in a massive increase in parasitemia and causes many of the symptoms associated with malaria infections, which can ultimately lead to death if left untreated.[3]

A majority of research in antimalarial drug discovery has focused on small molecules that affect parasite growth in the blood stage, which has heralded numerous successes. However, difficulties in administration in endemic regions and resistance to multiple therapeutics,[4−6] including the current gold standard artemisinin,[7,8] have necessitated the search for novel chemical scaffolds to combat this disease. There is a strong impetus to identify compounds that have new molecular targets, to which parasite populations would have no inherent resistance. While compound libraries, such as the malaria box,[9] are valuable resources for druglike antimalarial chemical scaffolds, the limited structural diversity of such libraries may reduce the number of cellular targets that can be accessed using these approaches. Due to the vast structural diversity of natural products,[10] in conjunction with their historical successes as antimalarials, it has been suggested that they hold promise as the source for next-generation therapeutics for malaria.[11]

Marine natural products have become a well-established source of new bioactive lead compounds, which is exemplified by the growing representation of these compounds in preclinical or clinical trials.[12] The description of the first marine obligate actinomycete genus, *Salinispora*, and the subsequent full genome sequence of *Salinispora tropica* has provided molecular evidence for biosynthesis of chemically diverse compounds by marine bacteria.[13,14] Among these, the discovery and clinical advancement of the proteasome inhibitor salinosporamide A[15,16] has inspired continued research into marine natural products as a source of clinically relevant lead compounds. In addition to development as a therapeutic for multiple myeloma, salinosporamide A also exhibits antimalarial activity,[17] demonstrating the value of marine Actinobacteria for global health drug discovery.

As part of our platform for lead compound discovery against infectious disease targets, we screened our bacterially derived marine natural products library against *P. falciparum* in order to discover novel chemotypes with potentially new modes of action (MOAs) that may serve as starting points for next-generation antimalarials. From these screening efforts, we identified salinipostin A (**1**) as a structurally unique antimalarial with potent inhibition of *P. falciparum* growth (EC_{50} = 50 nM) and a high selectivity index (SI > 10^3) (Figure 1, Table 1). Salinipostin A is produced by a *Salinispora* sp. (GenBank:

Received: October 24, 2014
Published: January 13, 2015

DOI: 10.1021/jo5024409
J. Org. Chem. 2015, 80, 1312−1320

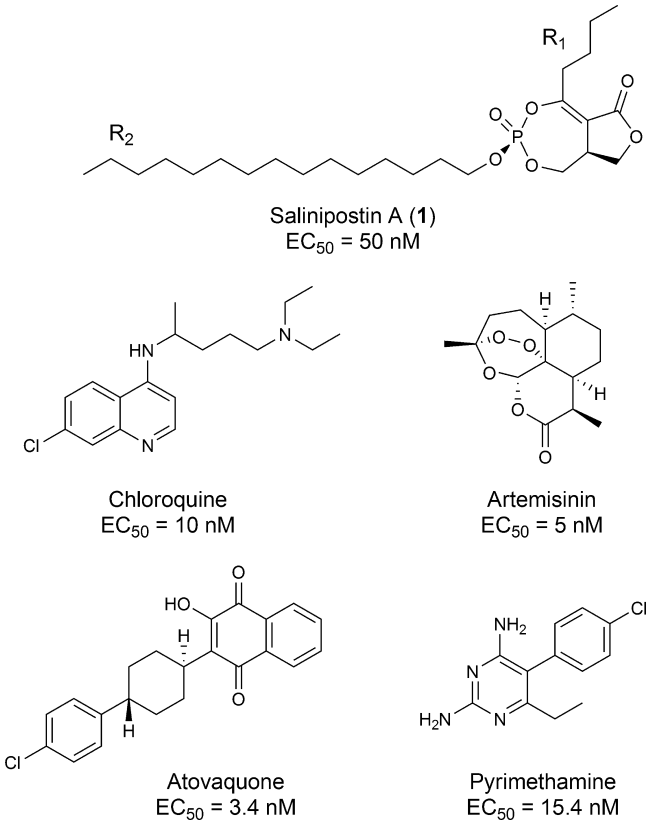

Figure 1. Structure of salinipostin A and other antimalarials.

Table 1. In Vitro Screening Results for Salinipostin A

cell type	EC_{50} (μM)
P. falciparum W2	0.05
HFF	>50
HEK-293T	>50
U2OS	>50
AsPC-1	>50

KP250536) isolated from a marine sediment sample and is a new example of the diversity of metabolites produced by this genus.[18] Further exploration into the biosynthetic potential of the producing organism uncovered 10 structurally related family members, salinipostins B–K (**2**–**11**). Screening of this library against *P. falciparum* revealed that relatively minor changes in chemical structure between analogues cause marked changes in potency. Due to the rare cyclic phosphotriester backbone of this molecule, the lack of structural similarity to any existing antimalarials, and the intriguing structural activity relationship (SAR) between analogues, we investigated the MOA of salinipostin A using a combination of microscopy and resistance selection assays. While these experiments were unable to definitively identify the molecular target, the results suggest that this compound class may be less susceptible to the facile development of resistance and indicate that further studies into the biological role(s) of this new class of compounds are warranted.

RESULTS AND DISCUSSION

Identification of salinipostins A–K. To identify novel antimalarial lead compounds, we screened our marine bacterially derived prefractionated natural products library against the chloroquine resistant W2 strain of *P. falciparum*. One of the prefractions, from a *Salinispora* sp., displayed potent activity against *P. falciparum* but did not cause growth inhibition or elicit a biologically active phenotype in HeLa cells in our cytological profiling assay.[19] Analysis of this prefraction by LCMS revealed a family of related compounds with mass differences of 14 amu, suggesting analogues with variable numbers of methylene or methyl groups (Figure S1, Supporting Information). These compounds were purified by reversed-phase (RP)-HPLC, and their activities were reassessed using the original assay conditions. These data identified salinipostin A (**1**) as the most potent compound against *P. falciparum* (EC_{50} = 50 nM). While the prefraction containing all of the salinipostins had previously not shown any activity against HeLa cells, salinipostin A was screened as a pure compound against an additional four mammalian cell lines. No significant growth inhibition was observed at a 1000-fold higher concentration than the EC_{50} in *P. falciparum* (Table 1 and Supporting Information). On the basis of this potency and selectivity, salinipostin A (**1**) was chosen as our lead candidate in follow-up biological studies.

Structure Elucidation of the Salinipostins. On the basis of the analysis of HRESITOFMS and NMR data, the molecular formula of salinipostin A was determined to be $C_{25}H_{45}O_6P$, giving the molecule five degrees of unsaturation. To determine the planar structure, extensive one- and two-dimensional NMR experiments were performed. Analysis of these data (gCOSY, TOCSY, gHSQC, and gHMBC) indicated that salinipostin A possessed three separate spin systems (Figure 2). The first

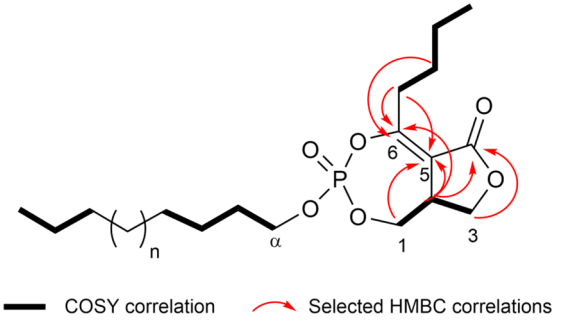

Figure 2. Structure elucidation of salinipostin A indicating key gCOSY and gHMBC correlations.

corresponded to a butyl chain that was determined to be allylic based on the chemical shifts of the terminal methylene protons at δ 2.79 and 2.97. The second spin system was revealed to be a saturated fatty alcohol chain, with multiple overlapping resonances in the methylene region. The final spin system consisted of one tertiary carbon flanked by two sets of diastereotopic methylenes on oxygenated secondary carbons. Key gHMBC correlations from this spin system to carbons with chemical shifts of δ 165.5, 168.9, and 110.3 revealed the presence of an α,β-unsaturated lactone. The protons from the butyl chain showed gHMBC correlations to carbons with chemical shifts of δ 168.9 and 110.3, allowing for the placement of this chain at the β-position of the lactone (Figure 2). The saturated alcohol chain was determined to be a pentadecyl alcohol based on integration of the ^{1}H spectrum and the remaining molecular formula of $C_{15}H_{31}O_2P$. With PO as the only unassigned atoms, and two remaining degrees of unsaturation, these three fragments were linked together

DOI: 10.1021/jo5024409
J. Org. Chem. 2015, 80, 1312–1320

Table 2. Biological Evaluation of Salinipostins A−K against *P. falciparum* W2

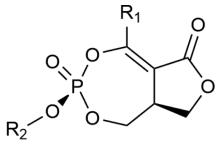

R_2 \ R_1				
$C_{15}H_{31}$	0.050 μM Salinipostin A (**1**)	-	0.266 μM Salinipostin F (**6**)	0.126 μM Salinipostin I (**9**)
$C_{14}H_{29}$	0.139 μM Salinipostin B (**2**)	0.082 μM Salinipostin D (**4**)	1.52 μM Salinipostin G (**7**)	49.6 μM Salinipostin J (**10**)
$C_{13}H_{27}$	0.415 μM Salinipostin C (**3**)	3.22 μM Salinipostin E (**5**)	8.70 μM Salinipostin H (**8**)	32.0 μM Salinipostin K (**11**)

through a cyclic phosphotriester, resulting in the full planar structure of salinipostin A as shown in Figure 2. The presence of the phosphorus atom was verified by ^{31}P NMR, which revealed a single resonance at δ −12.05 ppm, consistent with that of a phosphate triester.[20] The placement of the phosphotriester at this position was corroborated by the presence of both $^{2}J_{CP}$ and $^{3}J_{CP}$ coupling to neighboring carbon atoms C-1, C-5, C-6, and C-α (Figure S2, Supporting Information). While the length of the pentadecyl chain was calculated based on the molecular formula and integration of the ^{1}H NMR spectrum, this assignment was subsequently verified by MS/MS fragmentation. Fragmentation of the fatty alcohol chain allowed for the simultaneous determination of the mass of the saturated carbon chain and the bicyclic phosphotriester core (Figure S3, Supporting Information).

Characterization of the remaining analogues was accomplished by a similar analysis of one- and two-dimensional NMR experiments. On the basis of ^{1}H NMR data, it was determined that all of the analogues contained a bicyclic phosphotriester core identical to salinipostin A. The proton chemical shifts of all analogues associated with the core were identical within 0.01 ppm, and had very similar coupling constants (Table S1, Supporting Information). These results suggest that the biosynthetic machinery producing the bicyclic phophotriester core is producing exclusively one diastereomer. Utilizing gCOSY data, we determined that the structural variability between analogues arose from differing chain lengths in R_1 and R_2 (Table 2). The R_1 and R_2 assignments were assigned using a combination of gCOSY and HRESITOFMS data and validated using MS/MS fragmentation experiments to confirm these assignments. The MS/MS data corroborated the gCOSY and HRESITOFMS derived assignments (Figure S3, Supporting Information), definitively assigning the structures of salinipostins B−K as depicted in Table 2. Interestingly, many of these compounds possess odd chain lengths at R_2, in contrast to the even chain lengths more commonly encountered in traditional fatty acid biosynthesis. A number of marine organisms are known to produce odd chain fatty acids,[21] as are some bacterial species including *E. coli*, which is able to incorporate propionate as the starter unit rather than acetate during the initiation of chain elongation.[22] As will be seen below, this chain length variation contributes to the observed SAR pattern, and is an important feature of the structures of these new metabolites with respect to their antimalarial properties.

Configurational assignment of salinipostin A. Although the bicyclic phosphotriester core is a rare motif in natural products, the salinipostins share this structural feature with two other families of compounds, the cyclipostins and cyclophostins.[23−25] However, variations in the alkyl chain lengths at both R_1 and R_2, make the salinipostins constitutionally different to any members of either of these families. The cyclipostins, which also contain long chain phosphate esters, are potent inhibitors of hormone sensitive lipase (HSL) and have been shown to have antimycobacterial properties.[25,26] To date, neither of these families has been reported to possess any activity against *P. falciparum*. In addition to having different carbon skeletons, there are noticeable discrepancies in the comparison of the carbon and proton chemical shifts, as well as the coupling constants between these two compound classes and the salinipostins (Figure S2). We hypothesized that these disparities were due to configurational differences between the salinipostins and these other natural products.

In order to determine the absolute configuration of salinipostin A, we conducted vibrational circular dichroism (VCD) experiments. This method has been successful in determining the absolute stereochemistry of a number other natural products where more classical methods were not possible, or material was limited.[27−30] Comparison of experimental VCD analysis of salinipostin A with calculated VCD spectra for the lowest energy conformers of two diastereomers of the bicyclic core of the salinipostin scaffold (S_P,S_C and R_P,S_C, performed by BioTools, Inc.), carried out at the DFT level (B3LYP functional/6-31G(d) basis set) with Gaussian 09, revealed the absolute configuration of salinipostin A to be S_P,S_C (Figure S4). This assignment was determined by comparing the statistical fit of the experimental VCD spectrum

DOI: 10.1021/jo5024409
J. Org. Chem. 2015, 80, 1312−1320

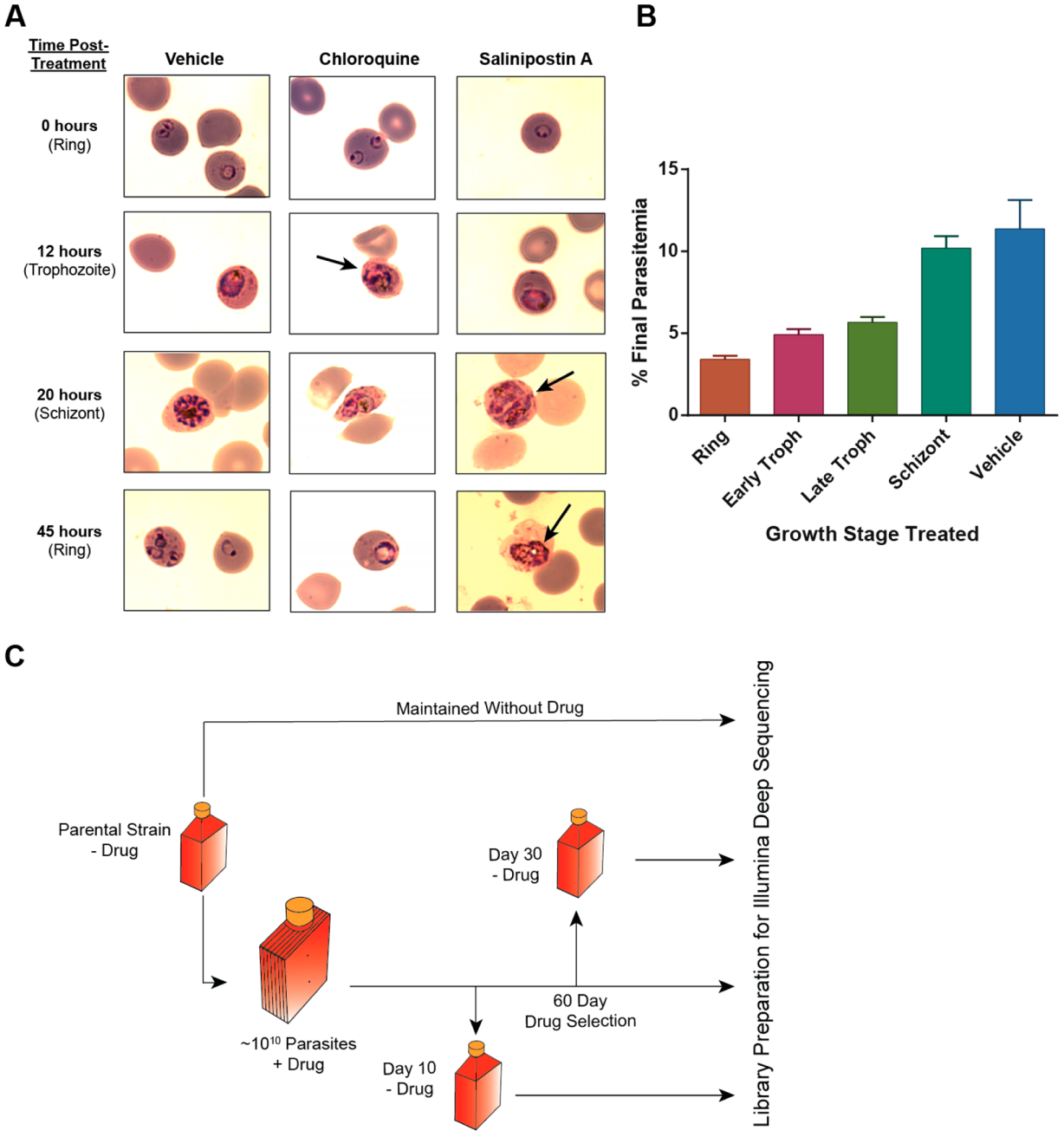

Figure 3. Biological effects of salinipostin A. (A) *P. falciparum* microscopy. (B) Parasitemia after salinipostin A treatment at various life stages. (C) Flowchart of resistance selection strategy for target identification.

with the calculated VCD spectra for all lowest energy conformers for each of the calculated diastereomers. Based on the overall better agreement in VCD pattern to the Botlzmann sum of the calculated spectra of the S_P,S_C than the R_P,S_C configuration, and the fact that the alignment of the S_P,S_C spectra were an absolute match, rather than a mirror image, the absolute configuration of salinipostin A was assigned as S_P,S_C. The remaining salinipostin family members were also assigned as S_P,S_C based on their shared biosynthetic origin and close agreement of spectroscopic data for the salinipostin core structure. This absolute configuration differs from that of the cyclipostins and the cyclophostins, which both possess an S_P,R_C configuration. Recently, the S_P,S_C diastereomer of cyclipostin P was prepared via total synthesis.[20] Comparison of the of the ^{31}P, ^{13}C, and ^{1}H NMR chemical shifts, and the $^{3}J_{CP}$ coupling constants between each of the diastereomers of the synthetic compounds with salinipostin A corroborated the relative configurations of the two chiral centers as corresponding to the S_P,S_C assignment of salinipostin A determined from VCD measurements (Figure S2).

Biological Evaluation and Structure–Activity Relationships of Salinipostins A–K against *P. falciparum*. Pure compound screening of salinipostins A–K against parasites revealed a broad range of EC_{50} values, extending from 50 nM to approximately 50 μM, equating to an approximate 1000-fold difference in activity between family members (Table 2). This drastic change in potency was striking, given that all of the salinipostins share the same bicyclic phosphotriester core and only differ in the length of aliphatic chains R_1 and R_2. Examination of the SAR data reveals

DOI: 10.1021/jo5024409
J. Org. Chem. 2015, 80, 1312–1320

two clear trends. First, an increase in activity is observed as the length of R_2 increases. In each series of R_1 (ethyl, propyl, isobutyl, butyl), the pentadecyl phosphoester at the R_2 position (**1**, **6**, **9**) is the most potent analogue. Second, there is also an increase in potency as the number of carbons in the vinyl aliphatic chain (R_1) increases. In the cases where R_1 is isobutyl (**4**, **5**), there is a slight decrease in activity in comparison to the straight chain butyl analogues (**1**−**3**); however, these analogues are more potent than when R_1 is propyl (**6**−**8**) (Table 2). This suggests that branching at the R_1 position slightly attenuates activity but supports the trend that longer chain lengths at this position increase potency. The isobutyl analogue with the pentadecyl phosphoester chain was not produced in high enough titer for structural characterization or biological screening.

Although it is unclear whether either of these structural features is singularly driving the variations in activity, it is apparent that the combination of both alkyl chain lengths results in drastic changes in potency. This is best exemplified by examining the differences in EC_{50} values between salinipostin K (**11**, EC_{50} = 32.0 μM) and salinipostin A (**1**, EC_{50} = 0.050 μM). The discrimination of alkyl chain lengths in biological systems is observed for fatty acid synthase inhibitors as well as post-translational modifications of proteins, such as palmitoylation.[31,32] This change in potency between analogues with relatively slight structural differences, coupled with the lack of cytotoxicity to mammalian cells, prompted us to further investigate the mode of action of salinipostin A in *P. falciparum* parasites.

Morphological Effects of Salinipostin A Treated Parasites. Morphological effects were clearly observed in W2 parasites treated with 6X EC_{90} (2.7 μM) salinipostin A during a 45-h life cycle; these effects were markedly different from the vehicle control (Figure 3A). Furthermore, parasites treated with salinipostin A appeared to show stage-specific growth arrest, which was delayed compared to the growth arrest of parasites treated with 6X EC_{90} chloroquine (10.8 μM). Treatment with salinipostin A was carried out alongside treatment with chloroquine, as the mode of action of chloroquine is well understood.[33] Antimalarial activity of chloroquine occurs by blocking polymerization and subsequent detoxification of heme molecules resulting from parasitic digestion of hemoglobin in the digestive vacuole of the parasite. As hemoglobin ingestion and subsequent digestion begins during the trophozoite stage, we expected to observe chloroquine treatment taking effect at 12 h; our results showed parasites with enlarged digestive vacuoles and an abundance of heme at this time point (Figure 3A). By contrast, salinipostin A-treated parasites did not present any observable morphological changes at 12 h compared to vehicle control. However, at 20 h we did see growth arrest and changes in parasite morphology for salinipostin A-treated cultures. Unlike chloroquine treatment, where it was evident that the overaccumulation of heme was producing toxic effects, parasites treated with salinipostin A appeared to lose cellular organization and experience general disintegration of internal structures when compared to the control (Figure 3A). At 45 h, reinvasion was seen in control cultures but not in cultures treated with chloroquine or salinipostin A. While these results do not pinpoint a mode of action for salinipostin A, they do reveal clear morphological and developmental changes for salinipostin A that are distinct from those for chloroquine.

Growth Stage Specificity. In order to examine the growth stage specificity of salinipostin A, we elected to perform wash in/wash out experiments at key stages of the *P. falciparum* lifecycle. Incubating specific stages of parasite growth in 3X EC_{90} of salinipostin A for 2 h followed by washing out the compound with normal media indicated that salinipostin A was not equally effective for all growth stages assayed, but rather was stage-specific over a 72-h period. Compared to vehicle control, early stages exhibited the highest sensitivity to salinipostin A, (Figure 3B) with ring stage showing the most drastic effect (3.4% parasitemia at 72 h). Both early-trophozoite and late-trophozoite stages were growth-inhibited by salinipostin A to a somewhat lesser degree with 4.9% parasitemia and 5.7% parasitemia at 72 h, respectively. The inhibitory effect of salinipostin A on schizont stage was minimal, and similar to vehicle control (10.2% parasitemia at 72 h). This latter observation, together with our microscopy work, suggests that salinipostin A disrupts a process required for the establishment or growth of the intracellular parasite, rather than a late-stage function, such as merozoite formation or invasion.

Attempts To Select for Resistant *P. falciparum* Mutants. One approach to target identification in eukaryotic parasites is the generation of resistant parasite populations using various levels of drug pressure and identification of the single nucleotide polymorphisms (SNPs) in the mutants that confer resistance by whole genome sequencing (Figure 3C). These mutations can be changes in drug efflux pumps, such as in chloroquine and mefloquine resistance.[6,34] Alternatively, mutations may also be copy number variants of the molecular target, or point mutations in the molecular target of the drug. This strategy has recently been implemented to identify drug targets or confirm determinants of resistance in *Plasmodium* for numerous molecules including fosmidomycin,[35] the spiroindolones,[36] thiaisoleucine,[37] benzothiazepines,[38] and cladosporin[39] and the dihydroisoquinolones.[40]

We attempted three separate resistance selections using a starting population of 10^{10} parasites and continuous drug pressure over 45 days each, at the EC_{95} (360 nM), EC_{90} (344 nM), and EC_{85} (160 nM) of salinipostin A. In each case, at the conclusion of the period of drug pressure, small numbers of viable parasites remained in the culture. None of these new populations exhibited a statistically significant shift in EC_{50} values, suggesting a small fraction of parasites escaped the lethal effects of the drug at these concentrations, rather than developed resistance.

It is unclear why this strategy to generate resistant parasites was unsuccessful for salinipostin A. It is possible that even more stringent selections at higher initial parasite populations and drug concentrations might result in the acquisition of resistance mutations. Alternatively, salinipostin A may exhibit antimalarial activity via a more general mechanism, such as membrane disruption; however, the selectivity for longer chain lengths in the SAR data suggests a more specific target. Another potential explanation is that salinipostin A affects post-translation protein modifications, such as lipidation. Considering this scenario, it would be unlikely that mutations in a single protein would confer resistance, which raises the intriguing possibility that these compounds may be less susceptible to the development of native resistance in the clinic than several of the existing therapeutics.

DOI: 10.1021/jo5024409
J. Org. Chem. 2015, 80, 1312−1320

CONCLUSION

Examination of our marine natural products library has led to the discovery of salinipostins A−K as potent antimalarial agents with high selectivity indices over tested mammalian cell lines. Application of a combination of NMR and VCD methods determined the absolute configuration of the core scaffold as S_P,S_C, in contrast to other structurally related natural products, all of which possess the S_P,R_C configuration. Subsequent examination of the biological attributes of salinipostin A indicated that compound treatment exerts a stage-specific arrest of parasite development and that there is a clear and strong structure−activity relationship within the series, with alkyl chain length having a profound effect on antimalarial potency. Finally, resistance selection experiments failed to generate resistant mutants under three independent selection conditions, suggesting that this new compound class may target an essential process of *Plasmodium* development that is not easily compensated by single protein changes and providing incentive for the development of chemical probes using this scaffold to identify new druggable targets in malaria.

EXPERIMENTAL SECTION

General Experimental Methods. Solvents used for HPLC chromatography were HPLC grade and were used without further purification. Optical rotations were measured using a 10 mm path length cell at 589 nm. NMR spectra were acquired on a 600 MHz spectrometer equipped with a 5 mm HCN triple resonance cryoprobe and referenced to residual solvent proton and carbon signals (δH 7.26, δC 77.16 for chloroform-*d*). High-resolution mass spectrometry data were acquired using an electrospray ionization (ESI) accurate-mass time-of-flight (TOF) liquid chromatograph−mass spectrometer.

Isolation, Fermentation, and Extraction of *Salinispora* sp. The producing organism, RL08-036-SPS-B, was isolated from a marine sediment sample collected by SCUBA near Keawekaheka Bay, HI, at a depth of 15 m. The strain was originally isolated on SPS medium (18.0 g of agar, 5.0 mg of polymixin B sulfate, 50.0 mg of nalidixic acid, 50.0 mg of cycloheximide, 750 mL of 0.2 μm filtered seawater, 250 mL of Milli-Q water) and further isolation performed on MB medium (37.4 g of Difco Marine Broth, 18 g of agar, 1 L of Milli-Q water). Analysis of the 16S rDNA sequence (GenBank: KP250536) identified this strain as a *Salinispora* sp., with highest sequence similarities to multiple *S. pacifica* strains (99% identity). The pure culture was cultivated on a rotary shaker (200 rpm, 27 °C) in 2.8 L Fernbach flasks containing 1 L of modified SYP medium (10.0 g of starch, 4.0 g of peptone 2.0 g of yeast extract, 31.2 g of Instant Ocean sea salt, 1.0 L of Milli-Q water) and a stainless steel spring. After 6 days, 20.0 g of Amberlite XAD-16 adsorbent resin was added, and the culture was allowed to shake for 2 h. The cells and resin were removed by vacuum filtration using Whatman glass microfiber filters and washed with deionized water. The resin and cells were extracted with 250 mL of 1:1 methanol/dichloromethane, and the organic extract was removed from the cells and resin by vacuum filtration and concentrated to dryness in vacuo. The crude organic extract, given extract code RLUS1359, was subjected to solid-phase extraction (SPE) using a Supelco-Discovery C_{18} cartridge (10 g) and eluted using a step gradient of 80 mL of MeOH/H_2O solvent mixtures (10% MeOH, 20% MeOH, 40% MeOH, 60% MeOH, 80% MeOH, 100% MeOH) and finally with ethyl acetate to afford seven fractions. The 10% MeOH fraction was discarded, and the remaining six were dried in vacuo. Analysis by RP-LCMS revealed the salinipostins were present only in the 100% MeOH fraction (RLUS1359E).

Purification of the Salinipostins. Prefraction RLUS1359E was separated into two subfractions using RP-HPLC (Phenomenex Synergi Fusion-RP 10 μm, 80 A, 250 × 4.6 mm, 82% to 93% MeOH/H_2O + 0.02% formic acid over 14 min, 2 mL min^{-1} flow rate). These two fractions (F1 and F2) were further purified by RP-HPLC to afford salinipostins A−K (F1: Phenomenex Kinetex XB-C_{18}, 2.6 μm, 100 A, 100 × 4.6 mm, 84%−85% MeOH/H_2O + 0.02% formic acid over 8 min, 1.2 mL min^{-1} flow rate, salinipostin K (**11**) t_R = 6.01 min, yield 40 ng/L; salinipostin H (**8**) t_R = 7.48 min, yield 9 ng/L; salinipostin J (**10**) t_R = 8.26 min, yield 14 ng/L; salinipostin E (**5**) t_R = 9.04 min, yield 31 ng/L; salinipostin C (**3**) t_R = 9.27 min, yield 390 ng/L; salinipostin G (**7**) t_R = 9.71 min, yield 56 ng/L F2: Phenomenex Kinetex XB-C_{18}, 2.6 μm, 100 A, 100 × 4.6 mm, 87%−88% MeOH/H_2O + 0.02% formic acid over 10 min, 1.2 mL min^{-1} flow rate, salinipostin I (**9**) t_R = 4.93 min, yield 7 ng/L salinipostin D (**4**) t_R = 5.27 min, yield 8 ng/L; salinipostin B (**2**) t_R = 5.44 min, 83 ng/L; salinipostin F (**6**) t_R = 5.84 min, 18 ng/L; salinipostin A (**1**) t_R = 7.05 min, 200 ng/L).

Chemical Characterization of Compounds. *Salinipostin A (**1**):* $[\alpha]^{25}_D$ +0.04 (*c* 0.075, MeOH); UV (MeOH) λ_{max}(log ε) 227 (3.39) nm; ^{1}H NMR ($CDCl_3$, 600 MHz) 4.44 (1H, dd, *J* = 9.3, 9.3 Hz), 4.28 (1H, d, *J* = 6.2 Hz), 4.18 (2H, t, *J* = 6.6 Hz), 4.03 (1H, m), 4.03 (1H, m), 3.78 (1H, dd, *J* = 5.5, 9.7 Hz), 2.97 (1H, dt, *J* = 7.7, 14.9 Hz), 2.79 (1H, dt, *J* = 5.5, 9.7 Hz), 1.72 (2H, p, *J* = 6.9 Hz), 1.58 (2H, p, *J* = 7.56), 1.39 (2H, m), 1.38 (2H, m), 1.33−1.22 (22H, m), 0.93 (3H, t, *J* = 7.3 Hz), 0.88 (3H, t, *J* = 7.0 Hz); ^{13}C NMR ($CDCl_3$, 151 MHz) δ 168.9, 165.4, 110.3, 69.7, 69.4, 64.6, 38.5, 30.4, 30.3, 29.8−29.2 (11C), 28.6, 25.4, 22.3, 14.2, 13.9; HRESIMS *m*/*z* 495.2852 [M + Na]$^+$ (calcd for $C_{25}H_{45}O_6PNa$, 495.2851).

*Salinipostin B (**2**):* $[\alpha]^{25}_D$ +0.01 (*c* 0.175, MeOH); UV (MeOH) λ_{max}(log ε) 229 (2.45) nm; ^{1}H NMR ($CDCl_3$, 600 MHz) 4.43 (1H, dd, *J* = 9.2, 9.2 Hz), 4.30 (1H, d, *J* = 6.2 Hz), 4.17 (2H, t, *J* = 7.0 Hz), 4.03 (1H, m), 4.03 (1H, m), 3.78 (1H, dd, *J* = 5.0, 9.7 Hz), 2.97 (1H, dt, *J* = 7.7, 14.7 Hz), 2.79 (1H, dt, *J* = 7.5, 14.3 Hz), 1.72 (2H, p, *J* = 6.9 Hz), 1.58 (2H, p, *J* = 7.8), 1.39 (2H, m), 1.38 (2H, m), 1.33−1.22 (20H, m), 0.98 (3H, t, *J* = 7.3 Hz), 0.88 (3H, t, *J* = 6.9 Hz); ^{13}C NMR ($CDCl_3$, 151 MHz) δ 168.9,165.4, 110.3, 69.7, 69.4, 64.6, 38.5, 30.4, 30.3, 29.8−29.1 (10C), 28.6, 25.4, 22.3, 14.2, 13.9; HRESIMS *m*/*z* 481.2694 [M + Na]$^+$ (calcd for $C_{24}H_{43}O_6PNa$, 481.2695).

*Salinipostin C (**3**):* $[\alpha]^{25}_D$ +0.03 (*c* 0.25, MeOH); UV (MeOH) λ_{max}(log ε) 230 (3.24) nm; ^{1}H NMR ($CDCl_3$, 600 MHz) 4.44 (1H, dd, *J* = 8.9, 8.9 Hz), 4.30 (1H, d, *J* = 6.2 Hz), 4.18 (2H, t, *J* = 6.9 Hz), 4.03 (1H, m), 4.03 (1H, m), 3.78 (1H, dd, *J* = 4.8, 9.8 Hz), 2.97 (1H, dt, *J* = 7.7, 14.7 Hz), 2.79 (1H, dt, *J* = 7.7, 14.3 Hz), 1.72 (2H, p, *J* = 6.7 Hz), 1.58 (2H, p, *J* = 8.0), 1.39 (2H, m), 1.38 (2H, m), 1.33−1.22 (18H, m), 0.93 (3H, t, *J* = 7.3 Hz), 0.88 (3H, t, *J* = 6.9 Hz); ^{13}C NMR ($CDCl_3$, 151 MHz) δ 168.9, 165.4, 110.3, 69.7, 69.4, 64.6, 38.5, 30.4, 30.3, 29.2−29.8 (9C), 28.6, 25.4, 22.3, 14.2, 13.9; HRESIMS *m*/*z* 467.2538 [M + Na]$^+$ (calcd for $C_{23}H_{41}O_6PNa$, 467.2538).

*Salinipostin D (**4**):* $[\alpha]^{25}_D$ +0.02 (*c* 0.06, MeOH); UV (MeOH) λ_{max}(log ε) 228 (2.92) nm; ^{1}H NMR ($CDCl_3$, 600 MHz) 4.44 (1H, dd, *J* = 9.2, 9.2 Hz), 4.32 (1H, d, *J* = 6.3 Hz), 4.17 (2H, t, *J* = 6.9 Hz), 4.03 (1H, m), 4.03 (1H, m), 3.78 (1H, dd, *J* = 5.4, 9.5 Hz), 2.91 (1H, dd, *J* = 7.3, 13.5 Hz), 2.66 (1H, dt, *J* = 7.3, 13.6 Hz), 2.06 (1H, hept, *J* = 6.7), 1.72 (2H, p, *J* = 7.0 Hz), 1.36 (2H, p, *J* = 6.8), 1.33−1.22 (20H, m), 0.99 (3H, t, *J* = 6.6 Hz), 0.97 (3H, t, *J* = 6.7 Hz), 0.88 (3H, t, *J* = 6.9 Hz); HRESIMS *m*/*z* 459.2870 [M + H]$^+$ (calcd for $C_{24}H_{44}O_6P$, 459.2876).

*Salinipostin E (**5**):* $[\alpha]^{25}_D$ +0.16 (*c* 0.01, MeOH); UV (MeOH) λ_{max}(log ε) 229 (4.02) nm; ^{1}H NMR ($CDCl_3$, 600 MHz) 4.44 (1H, dd, *J* = 9.1, 9.1 Hz), 4.33 (1H, d, *J* = 6.3 Hz), 4.18 (2H, t, *J* = 6.8 Hz), 4.03 (1H, m), 4.03 (1H, m), 3.78 (1H, dd, *J* = 5.4, 9.6 Hz), 2.91 (1H, dd, *J* = 7.3, 13.5 Hz), 2.66 (1H, dt, *J* = 7.3, 13.5 Hz), 2.06 (1H, hept, *J* = 6.9), 1.72 (2H, p, *J* = 6.7 Hz), 1.37 (2H, p, *J* = 6.9), 1.33−1.22 (18H, m), 0.99 (3H, t, *J* = 6.8 Hz), 0.97 (3H, t, *J* = 6.7 Hz), 0.88 (3H, t, *J* = 6.8 Hz); HRESIMS *m*/*z* 445.2723 [M + H]$^+$ (calcd for $C_{23}H_{42}O_6P$, 445.2719).

*Salinipostin F (**6**):* $[\alpha]^{25}_D$ −0.05 (*c* 0.08, MeOH); UV (MeOH) λ_{max}(log ε) 227 (2.70) nm; ^{1}H NMR ($CDCl_3$, 600 MHz) 4.43 (1H, dd, *J* = 8.6, 8.6 Hz), 4.30 (1H, d, *J* = 6.4 Hz), 4.17 (2H, t, *J* = 6.9 Hz), 4.03 (1H, m), 4.03 (1H, m), 3.77 (1H, dd, *J* = 4.0, 9.5 Hz), 2.97 (1H, dt, *J* = 7.4, 14.3 Hz), 2.79 (1H, dt, *J* = 7.7, 14.3 Hz), 1.72 (2H, p, *J* = 6.7 Hz), 1.64 (2H, m), 1.37 (2H, m), 1.33−1.22 (22H, m), 0.97 (3H, t, *J* = 7.8 Hz), 0.87 (3H, t, *J* = 6.7 Hz); HRESIMS *m*/*z* 481.2687 [M + Na]$^+$ (calcd for $C_{24}H_{43}O_6PNa$, 481.2689).

DOI: 10.1021/jo5024409
J. Org. Chem. 2015, 80, 1312−1320

*Salinipostin G (**7**):* $[\alpha]^{25}_{D}$ +0.02 (*c* 0.05, MeOH); UV (MeOH) λ_{max}(log ε) 224 (3.01) nm; ^{1}H NMR ($CDCl_3$, 600 MHz) 4.44 (1H, dd, *J* = 9.2, 9.2 Hz), 4.31 (1H, d, *J* = 6.2 Hz), 4.18 (2H, t, *J* = 6.9 Hz), 4.03 (1H, m), 4.03 (1H, m), 3.78 (1H, dd, *J* = 5.3, 9.6 Hz), 2.96 (1H, dt, *J* = 6.5, 13.7 Hz), 2.78 (1H, dt, *J* = 7.6, 14.5 Hz), 1.72 (2H, p, *J* = 6.7 Hz), 1.65 (2H, p, *J* = 7.4 Hz), 1.37 (2H, m), 1.33−1.22 (20H, m), 0.98 (3H, t, *J* = 7.4 Hz), 0.88 (3H, t, *J* = 7.1 Hz); HRESIMS *m*/*z* 467.2532 [M + Na]+ (calcd for $C_{23}H_{41}O_6PNa$, 467.2533).

*Salinipostin H (**8**):* $[\alpha]^{25}_{D}$ +0.02 (*c* 0.09, MeOH); UV (MeOH) λ_{max}(log ε) 227 (2.81) nm; ^{1}H NMR ($CDCl_3$, 600 MHz) 4.44 (1H, dd, *J* = 9.3, 9.3 Hz), 4.31 (1H, d, *J* = 6.2 Hz), 4.18 (2H, t, *J* = 6.7 Hz), 4.03 (1H, m), 4.03 (1H, m), 3.78 (1H, dd, *J* = 5.3, 9.8 Hz), 2.95 (1H, dt, *J* = 7.6, 13.8 Hz), 2.78 (1H, dt, *J* = 7.4, 14.1 Hz), 1.72 (2H, p, *J* = 6.9 Hz), 1.64 (2H, p, *J* = 7.5 Hz), 1.37 (2H, m), 1.33−1.22 (18H, m), 0.98 (3H, t, *J* = 7.4 Hz), 0.88 (3H, t, *J* = 7.0 Hz); HRESIMS *m*/*z* 431.2561 $[M + H]^+$ (calcd for $C_{22}H_{40}O_6P$, 431.2563).

*Salinipostin I (**9**):* $[\alpha]^{25}_{D}$ +0.02 (*c* 0.11, MeOH); UV (MeOH) λ_{max}(log ε) 227 (3.12) nm; ^{1}H NMR ($CDCl_3$, 600 MHz) 4.44 (1H, dd, *J* = 9.2, 9.2 Hz), 4.30 (1H, d, *J* = 6.4 Hz), 4.18 (2H, t, *J* = 6.9 Hz), 4.03 (1H, m), 4.03 (1H, m), 3.78 (1H, dd, *J* = 5.3, 9.4 Hz), 2.96 (1H, dq, *J* = 7.4, 7.5 Hz), 2.85 (1H, dq, *J* = 7.5, 7.4 Hz), 1.72 (2H, p, *J* = 6.8 Hz), 1.36 (2H, p, *J* = 7.6 Hz), 1.33−1.22 (22H, m), 1.17 (3H, t, *J* = 7.5 Hz), 0.88 (3H, t, *J* = 7.0 Hz); HRESIMS *m*/*z* 445.2713 $[M + H]^+$ (calcd for $C_{23}H_{42}O_6P$, 445.2719).

*Salinipostin J (**10**):* $[\alpha]^{25}_{D}$ +0.01 (*c* 0.10, MeOH); UV (MeOH) λ_{max}(log ε) 223 (2.71) nm; ^{1}H NMR ($CDCl_3$, 600 MHz) 4.44 (1H, dd, *J* = 9.2, 9.2 Hz), 4.30 (1H, d, *J* = 6.4 Hz), 4.18 (2H, t, *J* = 7.0 Hz), 4.03 (1H, m), 4.03 (1H, m), 3.78 (1H, dd, *J* = 5.3, 9.4 Hz), 2.95 (1H, dq, *J* = 7.4, 7.4 Hz), 2.86 (1H, dq, *J* = 7.5, 7.5 Hz), 1.72 (2H, p, *J* = 6.9 Hz), 1.36 (2H, p, *J* = 7.2 Hz), 1.33−1.22 (20H, m), 1.17 (3H, t, *J* = 7.5 Hz), 0.88 (3H, t, *J* = 7.2 Hz); HRESIMS *m*/*z* 431.2565 $[M + H]^+$ (calcd for $C_{22}H_{40}O_6P$, 431.2563).

*Salinipostin K (**11**):* $[\alpha]^{25}_{D}$ +0.03 (*c* 0.09, MeOH); UV (MeOH) λ_{max}(log ε) 227 (3.39) nm; ^{1}H NMR ($CDCl_3$, 600 MHz) 4.44 (1H, dd, *J* = 9.3, 9.3 Hz), 4.30 (1H, d, *J* = 6.3 Hz), 4.18 (2H, t, *J* = 6.8 Hz), 4.03 (1H, m), 4.03 (1H, m), 3.78 (1H, dd, *J* = 5.6, 9.6 Hz), 2.96 (1H, dq, *J* = 7.5, 7.5 Hz), 2.85 (1H, dq, *J* = 7.5, 7.4 Hz), 1.72 (2H, p, *J* = 7.0 Hz), 1.36 (2H, p, *J* = 6.5 Hz), 1.33−1.22 (18H, m), 1.17 (3H, t, *J* = 7.5 Hz), 0.88 (3H, t, *J* = 7.0 Hz); HRESIMS *m*/*z* 417.2405 $[M + H]^+$ (calcd for $C_{21}H_{38}O_6P$, 417.2406).

Parasite Culture. *P. falciparum* parasites used in our selection studies were of a W2 (chloroquine resistant) background strain. Parasites were grown as previously described[41,42] in vitro at 37 °C/5% O_2/5% CO_2/90% N_2 in RPMI 1640 media containing 0.5% w/v Albumax II, 28 mM $NaHCO_3$, 0.1 mM hypoxanthine, 50 μg/L gentamycin, and 25 mM HEPES (pH 7.4). Parasites were cultured as necessary to maintain a 2% hematocrit and less than 10% parasitemia.

Primary Screen for Antimalarial Activity by SYBR Green I. In order to determine antimalarial activities for the primary screening library, a parasite growth-inhibition assay was run utilizing a 96-well format liquid handler, with all drug dilutions, additions of culture, and washes performed by the liquid handling unit. DMSO stock screening plates were first diluted 1:10 in DMSO. From this 1:10 diluted stock plate two replicate 96 well plates were prepared containing 10 μL of 1:10 diluted extract per well. Cultures of W2 parasites (>90% ring stage, synchronized by 5% sorbitol treatment) at 0.8% parasitemia and 2% hematocrit were prepared, and 190 μL per well of culture was added to each replicate 96-well plate to yield biological duplicates while further diluting the compound 1:20 (for a final 1X concentration). The first column and twelfth column of each 96-well plate with culture added served as our controls: the first column contained infected RBCs (iRBCs) at 0.8% parasitemia, 2% hematocrit in DMSO vehicle alone and served as our positive control, while the twelfth column containing RBCs alone at 2% hematocrit in DMSO vehicle and served as our negative control. Plates were incubated at 37 °C/5% O_2/5% CO_2/90% N_2 for 72 h. Following this incubation, all plates were removed from the incubator and washed with 1X PBS. This wash entailed removing 170 μL of culture media (keeping blood pellet undisturbed), replacing an equal volume of 1X PBS, and mixing to ensure the pellet was well washed. After this wash step, all plates were placed back into the incubator at 37 °C/5% O_2/5% CO_2/90% N_2. We then prepared a SYBR Green I Lysis Buffer to stain and detect the presence of *Plasmodium* nucleic acid. The lysis buffer was prepared as follows: Tris Base was added to 1L of cell culture water (20 mM final concentration), pH was adjusted to 7.5 via addition of HCl, EDTA was added (20 mM final concentration), saponin was added (0.008% w/v final), and Triton X-100 was added (0.08% w/v final). This lysis buffer was mixed thoroughly, vacuum-filtered, and stored at room temperature. SYBR Green (10,000X concentration, from Invitrogen) was then diluted 1:5000 into our lysis buffer. We then added 15 μL per well of SYBR Green I Lysis Buffer to 384 well assay plates (Black, Flat Bottom, Low Flange). Previously washed 96 well plates were removed from the incubator and 15 μL per well from the 96 well plates were added and mixed 1:1 with SYBR Green I Lysis Buffer in the 384 well assay plates. These plates were then read for fluorescence intensity at 485 nm excitation and 530 nm emission. We utilized a custom script to extrapolate the raw data from the fluorescence plate reader and output heatmaps showing relative potency of all compounds tested, along with efficacy of controls (output as a ratio of iRBCs to RBCs alone; a ratio with a value of 10 or higher is preferred). Following this initial screen for antimalarial activity, compounds identified as potent were further screened to determine EC_{50} values in *P. falciparum*.

EC_{50} Determination by YOYO1 Fluorescence Assay. To gauge an appropriate concentration of compound to use in our resistance selection studies, we determined compound EC_{50} on a W2 strain of parasites. Parasite culture (in RPMI media) at 0.8% parasitemia (>90% ring stage, synchronized by 5% sorbitol treatment) and 0.5% hematocrit was plated into a 96-well culture plate. Appropriate concentrations of salinipostin A (starting from a 10 mM stock in 100% DMSO) ranging from 0.02−50 μM were added to the parasites (final 0.5% DMSO). This concentration range, along with a positive control of iRBCs in solvent only and a negative control of uninfected RBCs in solvent only, was performed in technical triplicates. Chloroquine was used as a chemical positive control. After a 72-h incubation at 37 °C/5% O_2/5% CO_2/90% N_2, parasites were fixed with 1% formaldehyde and incubated at room temperature for 1 h. Following fixation, 50 nM YOYO1 (Molecular Probes, Carlsbad, CA) was added to parasites. Staining took place overnight at room temperature, protected from the light. *P. falciparum* growth inhibition was quantified by measuring fluorescence with a flow cytometer equipped with a multiwell plate reader with excitation and emission wavelength bands centered at 485 and 530 nm, respectively. Through the use of Flowjo software from Tree Star, Inc., background fluorescence from wells with uninfected RBCs only was subtracted from all other wells to yield fluorescence counts used in the analysis. Software from Graphpad Prism was used to plot fluorescence counts against the logarithm of drug concentrations. Curve-fitting by nonlinear regression (sigmoidal dose−response) and allowing for a variable slope (equation: Y = bottom + (top−bottom)/(1 + $10^{((LogIC50\text{-}X)\cdot HillSlope)}$)) yielded a drug concentration at which a 50% reduction was observed in fluorescence counts compared to solvent-only control wells of infected RBCs.[43]

Microscopy. *P. falciparum* parasites of the W2 background strain were grown as described above to maintain a 2% hematocrit and less than 10% parasitemia. Prior to visualizing effects of salinipostin A on parasite growth via microscopy, parasite cultures underwent two consecutive cycles of synchronization (5% sorbitol treatment). Once highly synchronous (>90% ring stage), parasites from the same culture were split equally into six separate cultures. Three sets of duplicate cultures were made to test three different conditions: salinipostin A at 6× EC_{90} (2.7 μM), chloroquine at 6× EC_{90} (10.8 μM), and DMSO vehicle control. Immediately after changing out normal media for media with drug or vehicle (0 h), aliquots were taken from each culture for blood smear. Parasites were visualized by Giemsa stain, and images were captured by camera. Following blood smear preparation, all cultures were placed back in the incubator until subsequent time-points. Additional time-points were taken at 12, 20, and 45 h to cover one complete lifecycle of W2 parasites. For each additional time-point, blood smears were prepared from each culture and visualized via Giemsa stain with images captured by camera.

DOI: 10.1021/jo5024409
J. Org. Chem. 2015, 80, 1312−1320

Drug Wash In−Wash Out. W2 parasites were synchronized by 5% sorbitol treatment until the culture was >90% ring stage. Once parasites were synchronous, the culture was split equally into 12 separate cultures with each culture at 0.8% parasitemia and 2% hematocrit. From these 12 cultures, 6 sets of duplicate cultures were made. From these 6 sets, 4 sets of duplicates were to be used for 4 different time-points covering one complete lifecycle of W2 parasites (ring stage, early trophozoite stage, late trophozoite stage, and schizont stage). The two remaining sets of duplicate cultures were to be used for DMSO vehicle control and RBCs-only control. At ring stage (0 h), the duplicate cultures specified for ring stage were treated with salinipostin A at 3X EC_{90} (1.35 μM) and incubated at 37 °C/5% O_2/5% CO_2/90% N_2 for 2 h. At the same time, duplicate cultures specified for DMSO vehicle control and RBCs-only control were both given DMSO vehicle and incubated for 72 h. After the 2-h incubation, media from the ring-stage cultures treated with salinipostin A was washed out and replaced with normal media. After changing media, cultures were returned to the incubator for 70 h. At 10 h, duplicate cultures specified for early trophozoite stage were treated with 3× EC_{90} salinipostin A and incubated for 2 h. Following incubation, drug-treated media was replaced with normal media and the cultures were returned to the incubator for 62 h. At 24 h, duplicate cultures specified for late trophozoite stage were treated with 3× EC_{90} salinipostin A and incubated for 2 h. Following incubation, drug-treated media was replaced with normal media and the cultures were returned to the incubator for 48 h. At the 40-h time-point, duplicate cultures specified for schizont stage were treated with 3× EC_{90} salinipostin A and incubated for 2 h. Following incubation, drug-treated media was replaced with normal media, and the cultures were returned to the incubator for 32 h. At the 72-h time-point, all cultures were diluted down to 0.5% hematocrit with normal media followed by fixation with 0.8% Formaldehyde and staining with 50 nM YOYO1. Staining took place overnight at room temperature, protected from the light. YOYO1 fluorescence was measured by collecting 30000 events with a flow cytometer with excitation and emission wavelength bands centered at 485 and 530 nm, respectively. Through the use of Flowjo software from Tree Star, Inc., background fluorescence from RBCs-only cultures was subtracted from all other cultures to yield the percent population from each culture that were fluorescing YOYO1. The percent population fluorescing YOYO1 from each culture was defined as percent parasitemia in the data analysis.

Toxicity Screening against Mammalian Cells. Screening was performed against four cell types: human foreskin fibroblasts (HFF), HEK293T (human kidney), U2OS (human osteosarcoma), and AsPC-1 (human pancreatic adenocarcinoma). The cells were seeded into opaque-walled clear bottom 96-well plates at an initial seeding density of 2500 cells per well in 100 μL of Dulbecco's Modified Eagle's medium (HFF, HEK293T, AsPC-1) or McCoy's 5A medium (U2OS) and incubated at 37 °C under 5% CO_2 for 18 h. After this incubation period for cell attachment, 1 μL of salinipostin A in DMSO (1% final DMSO concentration) was transferred into each well in 3-fold dilutions (50−0.206 μM). Each concentration was screened in triplicate for a given cell type. Vehicle controls (n = 10, 1% DMSO) and positive controls (n = 2, PR-171, proteasome inhibitor) were included for each cell type. The treated plates were incubated for 48 h at 37 °C under 5% CO_2.

Toxicity was assessed using the CellTiter-Blue Cell Viability Assay (Promega) per the manufacturer's instructions. This method relies on the metabolic reduction of reasazurin into highly fluorescent resorufin by viable cells. The amount of fluorescence from each well is linearly correlated to the number of viable cells in that well. Briefly, 10 μL of the CellTiter Blue reagent was added to each well, and the plates were incubated for an additional 4 h at 37 °C under 5% CO_2. After this incubation period, the fluorescence was measured using a BioTek Cytation 3 imaging reader at λ_{ex} 560 nm/ λ_{em} 590 nm. Data were normalized to the average of 10 vehicle control wells and subtracted from 1 to assess growth inhibition. Plots and standard errors were calculated using Graphpad Prism software (Figure S5, Supporting Information).

■ ASSOCIATED CONTENT

Supporting Information

HPLC trace for salinipostin A−K isolation; comparison of key NMR chemical shifts for salinipostin A, 2-epicyclipostin P and cyclipostin P; ^{1}H, ^{13}C, COSY, HSQC, HMBC, and ^{31}P NMR data and MS^2 data for salinipostin A; ^{1}H, ^{13}C, COSY, and MS^2 data for salinipostins B and C; ^{1}H, COSY, and MS^2 spectra for salinipostins D−K; VCD data for configurational determination of salinipostin A; NMR table for salinipostins A−K; growth curves for mammalian cell lines This material is available free of charge via the Internet at http://pubs.acs.org.

■ AUTHOR INFORMATION

Corresponding Authors

*E-mail: joe@derisilab.ucsf.edu.

*E-mail: rliningt@ucsc.edu.

Author Contributions

§These authors contributed equally to the manuscript.

Notes

The authors declare no competing financial interest.

■ ACKNOWLEDGMENTS

This work was supported in part by the Sandler Center for Drug Discovery. We thank C. P. Canlas for assistance with ^{31}P NMR measurements, R. S. Lokey for access to the UCSC Chemical Screening Center, and Dr. W.R. Wong for 16S sequencing analysis.

■ REFERENCES

(1) Sachs, J.; Malaney, P. *Nature* **2002**, *415*, 680−5.

(2) *World Malaria Report 2012*; World Health Organization: Geneva, Switzerland, 2012.

(3) Miller, L. H.; Ackerman, H. C.; Su, X. Z.; Wellems, T. E. *Nat. Med.* **2013**, *19*, 156−67.

(4) Sibley, C. H.; Hyde, J. E.; Sims, P. F.; Plowe, C. V.; Kublin, J. G.; Mberu, E. K.; Cowman, A. F.; Winstanley, P. A.; Watkins, W. M.; Nzila, A. M. *Trends Parasitol.* **2001**, *17*, 582−8.

(5) Korsinczky, M.; Chen, N.; Kotecka, B.; Saul, A.; Rieckmann, K.; Cheng, Q. *Antimicrob. Agents Chemother.* **2000**, *44*, 2100−2108.

(6) Djimdé, A.; Doumbo, O. K.; Cortese, J. F.; Kayentao, K.; Doumbo, S.; Diourté, Y.; Coulibaly, D.; Dicko, A.; Su, X. Z.; Nomura, T.; Fidock, D. A.; Wellems, T. E.; Plowe, C. V. *N. Engl. J. Med.* **2001**, *344*, 257−63.

(7) Phyo, A. P.; Nkhoma, S.; Stepniewska, K.; Ashley, E. A.; Nair, S.; McGready, R.; ler Moo, C.; Al-Saai, S.; Dondorp, A. M.; Lwin, K. M.; Singhasivanon, P.; Day, N. P.; White, N. J.; Anderson, T. J. C.; Nosten, F. *Lancet* **2012**, *379*, 1960−6.

(8) Cheeseman, I. H.; Miller, B. A.; Nair, S.; Nkhoma, S.; Tan, A.; Tan, J. C.; Al Saai, S.; Phyo, A. P.; Moo, C. L.; Lwin, K. M.; McGready, R.; Ashley, E.; Imwong, M.; Stepniewska, K.; Yi, P.; Dondorp, A. M.; Mayxay, M.; Newton, P. N.; White, N. J.; Nosten, F.; Ferdig, M. T.; Anderson, T. J. C. *Science* **2012**, *336*, 79−82.

(9) Spangenberg, T.; Burrows, J. N.; Kowalczyk, P.; McDonald, S.; Wells, T. N. C.; Willis, P. *PLoS One* **2013**, *8*, e62906.

(10) Lachance, H.; Wetzel, S.; Kumar, K.; Waldmann, H. *J. Med. Chem.* **2012**, *55*, 5989−6001.

(11) Wells, T. N. C. *Malar. J.* **2011**, *10* (Suppl 1), S3.

(12) Gerwick, W. H.; Moore, B. S. *Chem. Biol.* **2012**, *19*, 85−98.

(13) Maldonado, L. A.; Fenical, W.; Jensen, P. R.; Kauffman, C. A.; Mincer, T. J.; Ward, A. C.; Bull, A. T.; Goodfellow, M. *Int. J. Syst. Evol. Microbiol.* **2005**, *55*, 1759−66.

(14) Udwary, D. W.; Zeigler, L.; Asolkar, R. N.; Singan, V.; Lapidus, A.; Fenical, W.; Jensen, P. R.; Moore, B. S. *Proc. Natl. Acad. Sci. U.S.A.* **2007**, *104*, 10376−81.

DOI: 10.1021/jo5024409
J. Org. Chem. 2015, 80, 1312−1320

(15) Feling, R. H.; Buchanan, G. O.; Mincer, T. J.; Kauffman, C. A.; Jensen, P. R.; Fenical, W. *Angew. Chem., Int. Ed.* **2003**, *42*, 355−7.
(16) Potts, B. C.; Albitar, M. X.; Anderson, K. C.; Baritaki, S.; Berkers, C.; Bonavida, B.; Chandra, J.; Chauhan, D.; Cusack, J. C.; Fenical, W.; Ghobrial, I. M.; Groll, M.; Jensen, P. R.; Lam, K. S.; Lloyd, G. K.; McBride, W.; McConkey, D. J.; Miller, C. P.; Neuteboom, S. T.; Oki, Y.; Ovaa, H.; Pajonk, F.; Richardson, P. G.; Roccaro, A. M.; Sloss, C. M.; Spear, M. A.; Valashi, E.; Younes, A.; Palladino, M. A. *Curr. Cancer Drug Targets* **2011**, *11*, 254−84.
(17) Prudhomme, J.; McDaniel, E.; Ponts, N.; Bertani, S.; Fenical, W.; Jensen, P.; Le Roch, K. *PLoS One* **2008**, *3*, e2335.
(18) Ziemert, N.; Lechner, A.; Wietz, M.; Millán-Aguiñaga, N.; Chavarria, K. L.; Jensen, P. R. *Proc. Natl. Acad. Sci. U.S.A.* **2014**, *111*, E1130−9.
(19) Schulze, C. J.; Bray, W. M.; Woerhmann, M. H.; Stuart, J.; Lokey, R. S.; Linington, R. G. *Chem. Biol.* **2013**, *20*, 285−95.
(20) Malla, R. K.; Bandyopadhyay, S.; Spilling, C. D.; Dutta, S.; Dupureur, C. M. *Org. Lett.* **2011**, *13*, 3094−7.
(21) Ackman, R. G.; Sipos, J. C. *Comp. Biochem. Physiol.* **1965**, *15*, 445−56.
(22) Ingram, L. O.; Chevalier, L. S.; Gabba, E. J.; Ley, K. D.; Winters, K. *J. Bacteriol.* **1977**, *131*, 1023−5.
(23) Kurokawa, T.; Suzuki, K.; Hayaoka, T.; Nakagawa, T.; Izawa, T.; Kobayashi, M.; Harada, N. *J. Antibiot.* **1993**, *46*, 1315−8.
(24) Vértesy, L.; Beck, B.; Brönstrup, M.; Ehrlich, K.; Kurz, M.; Müller, G.; Schummer, D.; Seibert, G. *J. Antibiot.* **2002**, *55*, 480−94.
(25) Wink, J.; Schmidt, F. R.; Seibert, G.; Aretz, W. *J. Antibiot.* **2002**, *55*, 472−9.
(26) Seibert, G.; Toti, L.; Wink, J. Use of Cyclipostin Derivatives for the Treatment of Mycobacterial Infectious Diseases. 7,923,438, 2011.
(27) Stephens, P. J.; McCann, D. M.; Devlin, F. J.; Smith, A. B. *J. Nat. Prod.* **2006**, *69*, 1055−64.
(28) Hopmann, K. H.; Šebestík, J.; Novotná, J.; Stensen, W.; Urbanová, M.; Svenson, J.; Svendsen, J. S.; Bouř, P.; Ruud, K. *J. Org. Chem.* **2012**, *77*, 858−69.
(29) Cedrón, J. C.; Estévez-Braun, A.; Ravelo, A. G.; Gutiérrez, D.; Flores, N.; Bucio, M. A.; Pérez-Hernández, N.; Joseph-Nathan, P. *Org. Lett.* **2009**, *11*, 1491−4.
(30) He, Y.; Wang, B.; Dukor, R. K.; Nafie, L. A. *Appl. Spectrosc.* **2011**, *65*, 699−723.
(31) Morbidoni, H. R.; Vilchèze, C.; Kremer, L.; Bittman, R.; Sacchettini, J. C.; Jacobs, W. R. *Chem. Biol.* **2006**, *13*, 297−307.
(32) Jones, M. L.; Collins, M. O.; Goulding, D.; Choudhary, J. S.; Rayner, J. C. *Cell Host Microbe* **2012**, *12*, 246−58.
(33) Valderramos, S. G.; Valderramos, J.-C.; Musset, L.; Purcell, L. A.; Mercereau-Puijalon, O.; Legrand, E.; Fidock, D. A. *PLoS Pathog.* **2010**, *6*, e1000887.
(34) Wilson, C. M.; Volkman, S. K.; Thaithong, S.; Martin, R. K.; Kyle, D. E.; Milhous, W. K.; Wirth, D. F. *Mol. Biochem. Parasitol.* **1993**, *57*, 151−60.
(35) Dharia, N. V.; Sidhu, A. B. S.; Cassera, M. B.; Westenberger, S. J.; Bopp, S. E.; Eastman, R. T.; Plouffe, D.; Batalov, S.; Park, D. J.; Volkman, S. K.; Wirth, D. F.; Zhou, Y.; Fidock, D. A.; Winzeler, E. A. *Genome Biol.* **2009**, *10*, R21.
(36) Rottmann, M.; McNamara, C.; Yeung, B. K. S.; Lee, M. C. S.; Zou, B.; Russell, B.; Seitz, P.; Plouffe, D. M.; Dharia, N. V.; Tan, J.; Cohen, S. B.; Spencer, K. R.; González-Páez, G. E.; Lakshminarayana, S. B.; Goh, A.; Suwanarusk, R.; Jegla, T.; Schmitt, E. K.; Beck, H.-P.; Brun, R.; Nosten, F.; Renia, L.; Dartois, V.; Keller, T. H.; Fidock, D. A.; Winzeler, E. A.; Diagana, T. T. *Science* **2010**, *329*, 1175−80.
(37) Istvan, E. S.; Dharia, N. V.; Bopp, S. E.; Gluzman, I.; Winzeler, E. A.; Goldberg, D. E. *Proc. Natl. Acad. Sci. U.S.A.* **2011**, *108*, 1627−32.
(38) Dong, C. K.; Urgaonkar, S.; Cortese, J. F.; Gamo, F.-J.; Garcia-Bustos, J. F.; Lafuente, M. J.; Patel, V.; Ross, L.; Coleman, B. I.; Derbyshire, E. R.; Clish, C. B.; Serrano, A. E.; Cromwell, M.; Barker, R. H.; Dvorin, J. D.; Duraisingh, M. T.; Wirth, D. F.; Clardy, J.; Mazitschek, R. *Chem. Biol.* **2011**, *18*, 1602−10.
(39) Hoepfner, D.; McNamara, C. W.; Lim, C. S.; Studer, C.; Riedl, R.; Aust, T.; McCormack, S. L.; Plouffe, D. M.; Meister, S.; Schuierer, S.; Plikat, U.; Hartmann, N.; Staedtler, F.; Cotesta, S.; Schmitt, E. K.; Petersen, F.; Supek, F.; Glynne, R. J.; Tallarico, J. A.; Porter, J. A.; Fishman, M. C.; Bodenreider, C.; Diagana, T. T.; Movva, N. R.; Winzeler, E. A. *Cell Host Microbe* **2012**, *11*, 654−63.
(40) Jiménez-Díaz, M. B.; Ebert, D.; Salinas, Y.; Pradhan, A.; Lehane, A. M.; Myrand-Lapierre, M.-E.; O'Loughlin, K. G.; Shackleford, D. M.; Justino de Almeida, M.; Carrillo, A. K.; Clark, J. A.; Dennis, A. S. M.; Diep, J.; Deng, X.; Duffy, S.; Endsley, A. N.; Fedewa, G.; Guiguemde, W. A.; Gómez, M. G.; Holbrook, G.; Horst, J.; Kim, C. C.; Liu, J.; Lee, M. C. S.; Matheny, A.; Martínez, M. S.; Miller, G.; Rodríguez-Alejandre, A.; Sanz, L.; Sigal, M.; Spillman, N. J.; Stein, P. D.; Wang, Z.; Zhu, F.; Waterson, D.; Knapp, S.; Shelat, A.; Avery, V. M.; Fidock, D. A.; Gamo, F.-J.; Charman, S. A.; Mirsalis, J. C.; Ma, H.; Ferrer, S.; Kirk, K.; Angulo-Barturen, I.; Kyle, D. E.; DeRisi, J. L.; Floyd, D. M.; Guy, R. K. *Proc. Natl. Acad. Sci. U.S.A.* **2014**.
(41) Haynes, J. D.; Diggs, C. L.; Hines, F. A.; Desjardins, R. E. *Nature* **1976**, *263*, 767−9.
(42) Trager, W.; Jensen, J. B. *Science* **1976**, *193*, 673−5.
(43) Weisman, J. L.; Liou, A. P.; Shelat, A. A.; Cohen, F. E.; Guy, R. K.; DeRisi, J. L. *Chem. Biol. Drug Des.* **2006**, *67*, 409−16.

DOI: 10.1021/jo5024409
J. Org. Chem. 2015, 80, 1312−1320